Available online at www.sciencedirect.com
SCIENCE DIRECT®
Physica A 359 (2006) 48–64
PHYSICA A
www.elsevier.com/locate/physa

Effect of noise on the critical golden-mean quasiperiodic dynamics in the circle map

Alexander P. Kuznetsov[a], Sergey P. Kuznetsov[a,b,*], Julia V. Sedova[a]

[a]*Institute of Radio-Engineering and Electronics of RAS, Saratov Division, Zelenaya 38, Saratov 410019, Russian Federation*
[b]*Max-Planck-Institut für Physik Komplexer Systeme, Nöthnitzer Straße 38, 01187 Dresden, Germany*

Received 3 March 2005
Available online 15 June 2005

Abstract

Scaling regularities are examined associated with effect of additive noise on a critical circle map at the golden-mean rotation number. We present an improved numerical estimate for the scaling constant of Hamm and Graham (Phys. Rev. A46, (1992) 6323) responsible for the effect of noise, $\gamma = 2.3061852653$. Decrease of the noise amplitude by this number ensures possibility to distinguish one more level of fractal-like structure, associated with increase of characteristic time scale by the golden mean factor $(\sqrt{5}+1)/2$. Numeric results demonstrating evidence of the expected scaling are presented, e.g. portraits of the noisy attractors, devil's staircase plots, Lyapunov charts on the parameter plane in different scales.

PACS: 05.45.−a; 05.10.Cc; 05.40.Ca

Keywords: Circle map; Golden mean; Noise; Renormalization; Scaling

*Corresponding author.
E-mail addresses: kuznetsov@sgu.ru, alkuz@sgu.ru (A.P. Kuznetsov).

0378-4371/$ - see front matter © 2005 Elsevier B.V. All rights reserved.
doi:10.1016/j.physa.2005.05.002

1. Introduction

One of paradigmatic objects in the modern nonlinear dynamics is a one-dimensional circle map. This is not only a simple and convenient artificial system but also a productive model for description many phenomena in physics and other sciences. It relates, in particular, to self-oscillators driven by periodic force [1], Josephson junctions in microwave field [2,3], space-charge waves in solids [3], driven damped pendulum [4]. In studies concerning biological and medical problems the circle map appears as a model of heart dynamics e.g. in presence of competition of two pacemakers controlling the rhythm [5].

Moreover, the circle map must be regarded not only as a qualitative model, but it manifest universal quantitative regularities at the transition to chaos via quasiperiodic motion. It follows from the renormalization group (RG) approach [6], which is commonly recognized as an effective and powerful theoretical tool for analysis of deep and fundamental features of dynamics between order and chaos. In particular, it uncovers such a feature of dynamics as scale invariance (scaling) for subtle fractal structures in phase space and in parameter space associated with transitions to chaos. In nonlinear dynamics, the RG approach was introduced by Feigenbaum [7] in application to period doubling scenario of the onset of chaos. Latter it was applied successively for analysis of other types of transitions to chaos, including different period-doubling universality classes [8], intermittency [9], quasiperiodicity [10], phenomena of complex analytic dynamics [11], and transitions in coupled systems [12].

The most advanced results of theoretical studies and experiments on the onset of chaos via quasiperiodicity relate to the case of the golden-mean ratio of the basic involved frequencies, $(\sqrt{5}+1)/2$. Selection of this particular irrational is justified not only by a commonly recognized simplicity and transparency of the respective theoretical analysis, but also by a fact that in this case subtle structures in phase space and parameter space revealed in theoretical researches or in experiments are distinguishable better than those at other frequency ratios.

A number of accurate experimental studies were reported, in which many details of the golden-mean critical dynamics predicted by the RG analysis were carefully observed and documented, in particular, in fluid convection and in forced electronic oscillators [13]. It relates to details of the parameter space structures (Arnold tongues), scaling and multifractal properties of the critical quasiperiodic motion, Fourier spectra, etc.

It should be noted, however, that all real experimental systems inevitably contain intrinsic noise. Account of noise is a crucial matter in careful analysis of phenomena at the onset of chaos because the noise obviously blurs the most intimate details of the observed fractal-like structures. With respect to application of the circle map to description of Josephson junctions this circumstance was stressed e.g. in Ref. [14].

For description of effect of noise, the pioneering theoretical approach based on the RG analysis was suggested by Crutchfield et al. and Shraiman et al. [15] in application to period-doubling transition to chaos in dissipative systems. These authors determined a universal factor $\gamma_{\mathrm{PD}} = 6.619036\ldots$ responsible for the scaling properties of the transition in respect to the effect of noise. Namely, decrease of amplitude of noise with that factor ensures a possibility for observation of one more

level of the period doubling cascade. Latter, analogous studies were performed for other types of critical behavior at the onset of chaos [16–20]. In particular, in Ref. [16] Hamm and Graham developed the RG approach for the transition to chaos via the golden-mean quasiperiodicity in the circle map and estimated respective scaling factor for the effect of noise, $\gamma = 2.30619$. Decrease of the noise intensity by this factor gives a possibility to distinguish one more level of the fractal structure, associated with characteristic time scale increased by the golden mean factor $W = (\sqrt{5}+1)/2$. Beside that paper, we aware of only two works specially devoted to the effect of noise on the circle map [14,21]. They were published before the paper of Hamm and Graham and contain only empirical results of numerical simulations without solid RG foundation.

The aim of the present paper is to examine in more details scaling properties intrinsic to the circle map under effect of noise near the critical golden-mean quasiperiodic orbit, which follow from the RG approach. Section 2 is devoted to discussion of some empirical numerical results for a stochastic version of the circle map model with additive noise. In Section 3 we reproduce RG analysis of the effects of noise based on one of the approaches suggested by Hamm and Graham, and present an improved numerical value for the basic universal constant responsible for the scaling properties in respect to noise. In Section 4 conclusions following from the RG analysis are discussed in application to the circle map with noise. Computer illustrations for scaling regularities are presented including portraits of the noisy attractors, devil's staircase plots, gray-scale charts for the Lyapunov exponent on the parameter plane near the golden-mean critical point in different scales and at different noise levels.

2. Effect of noise: empirical results

As known [6,22], in the sine circle map

$$x_{n+1} = x_n + r - \frac{K}{2\pi}\sin\ 2\pi x_n \ (mod\ 1), \tag{1}$$

the critical quasiperiodic motion at the onset of chaos with rotation number $w = W^{-1} = (\sqrt{5}-1)/2$ occurs at

$$K_c = 1,\ r_c = 0.60661063470112012 28\ldots \tag{2}$$

We will refer to this as the golden meal critical point, or GM critical point.

Let us introduce a sequence ξ_n that represents a discrete-time white noise, i.e. the terms of this sequence are assumed to be statistically independent. The maximal magnitude of ξ_n is supposed to be bounded. The average for ξ_n is zero, $\langle \xi_n \rangle = 0$, the standard deviation is some constant, $\sigma = \sqrt{\langle \xi_n^2 \rangle}$. Now, we consider the following iterative stochastic map

$$x_{n+1} = x_n + r - \frac{k}{2\pi}\sin\ 2\pi x_n + \varepsilon\xi_n \ (mod\ 1), \tag{3}$$

where ε characterizes intensity of the additive noise source.

If amplitude of noise is small, and we examine behavior near the critical point on large time scales, the concrete form of the probability distribution for ξ_n apparently will be not essential, and the behavior of the noisy system will be of a universal nature. (The same is true for other critical situations allowing analysis in terms of the RG method, cf. Ref. [23].) In the present computations we define ξ_n as a random variable uniformly distributed over an interval $[-0.5, 0.5]$; hence, $\sigma = 1/\sqrt{12}$.

In Fig. 1 we show Lyapunov charts on the plane of control parameter λ versus amplitude of driving ε without noise ($\varepsilon = 0$) and in presence of noise ($\varepsilon = 0.03$). The Lyapunov exponent has been computed via relation

$$\Lambda \cong N^{-1} \sum \log |1 - K \cos(2\pi x_n)| \tag{4}$$

at each pixel of the picture. Negative values of Λ are coded in gray scale: the lighter the color, the less negative is the Lyapunov exponent. Zero Λ corresponding to quasiperiodic dynamics are designated by white, and positive ones associated with chaotic dynamics by black. Location of the GM critical point is indicated on the panel (a). (See Ref. [24] for idea and other examples of use of the Lyapunov charts.)

Domains of periodic behavior in the noiseless case known as Arnold tongues are clearly visible in the panel (b) as gray colored formations. Between them, in the subcritical domain $K<1$ quasiperiodic dynamics takes place.

In presence of noise, periodic or quasiperiodic dynamics in pure sense do not occur, but the Lyapunov charts clearly demonstrate that the picture similar to that of the noiseless map is visible at least at small or moderate noises, although subtle details fade away due to the noise. We may speak of noisy periodic regimes, if the Lyapunov exponent is essentially negative, or of noise quasiperiodic, if it is close to zero, or of noisy chaotic, if it is positive. The Lyapunov charts allow an easy visual recognition of them. Observe gradual disappearance of subtle structure of domains in the parameter plane with increase of noise level in diagrams (b)–(d).

Fig. 2 shows portraits of attractors at the GM critical point in coordinates x_{n+F_k} versus x_n, where F_k is one of Fibonacci numbers. (Concretely, diagrams in Fig. 2 have been plotted for $F_6 = 8$.) This form of graphical presentation of motions will be convenient in further considerations. Panel (a) corresponds to a pure dynamical case (no noise), panels (b)–(d) to presence of noise of subsequently increasing amplitudes. One can see how the picture of the attractor becomes blurred in higher and higher degree with increase of noise, and the subtle details step by step disappear on the noisy background.

3. Renormalization group analysis

In application to all situations of the golden-mean quasiperiodisity, the main idea of the RG analysis consists in examination of evolution operators defined for time intervals given by subsequent Fibonacci's numbers F_k: $F_0 = 0$, $F_1 = 1$, $F_{k+2} = F_{k+1} + F_k$.

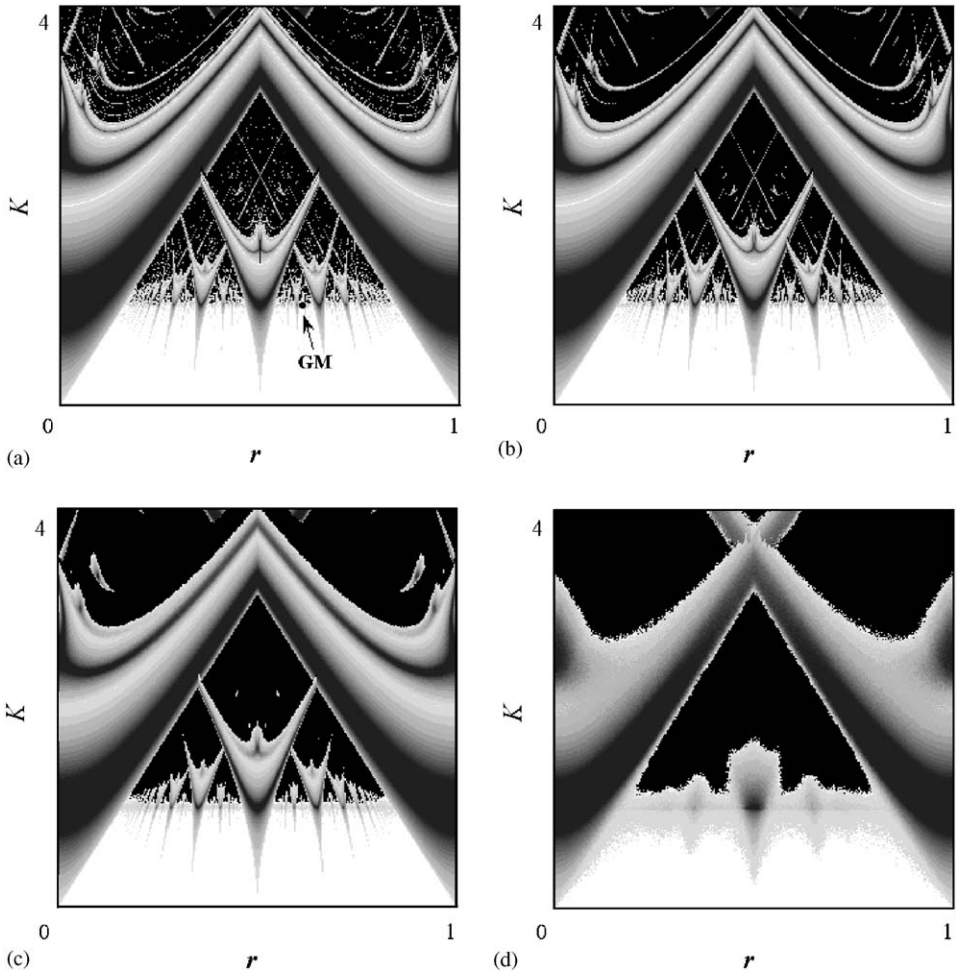

Fig. 1. Lyapunov charts for the map (3) on the plane of control parameters r and K. At each pixel of the pictures, the Lyapunov exponent computed from the expression (4) is coded in gray scale. Gray tones designate negative values of the Lyapunov exponent (the lighter the color, the less negative is the exponent). Zero values (quasiperiodic dynamics) are designated by white, and positive values (chaos) by black. Panel (a) corresponds to absence of noise ($\varepsilon = 0$), and the next panels to subsequently increasing intensity of noise, $\varepsilon = 0.001$ (b), $\varepsilon = 0.01$ (c) $\varepsilon = 0.1$ (d). On panel (a) location of the golden-mean critical point (2) is indicated as GM.

Let us suppose that in presence of noise evolution of the dynamical variable x at the GM point for F_k and F_{k+1} steps is governed by equations

$$x_{i+F_k} = \phi_k(x_i) + \varepsilon\xi_i\psi_k(x_i) \tag{5}$$

and

$$x_{i+F_k} = \phi_{k+1}(x_i) + \varepsilon\xi_i\psi_{k+1}(x_i), \tag{6}$$

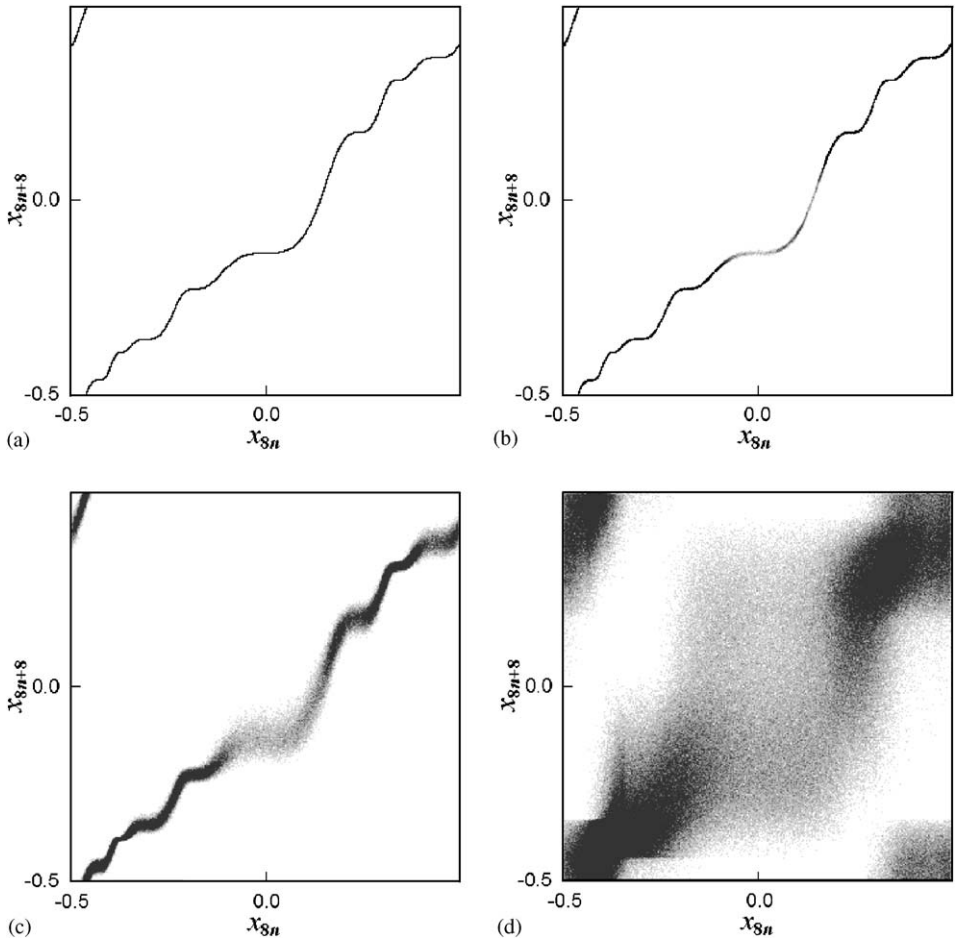

Fig. 2. Portraits of attractor at the GM critical point of the model (3) on iteration diagrams in coordinates $(x_n,\ x_{n+Fk})$ with $F_k = F_6 = 8$. Diagram (a) corresponds to a pure dynamical case (no noise), and other diagrams to presence of noise of subsequently increased amplitude: $\varepsilon = 0.001$ (b), $\varepsilon = 0.01$ (c) $\varepsilon = 0.1$ (d).

where ξ_i designates random numbers with properties formulated in the previous section, $\psi_k(x)$ and $\psi_{k+1}(x)$ are some auxiliary functions. The noise amplitude parameter ε is supposed to be small. Obviously, the model (3) represents a particular version of Eqs. (5) and (6): at $F_1 = F_2 = 1$ we set

$$\phi_1(x) = \phi_2(x) = x + r_c - (1/2\pi)\sin\ 2\pi x,\ \psi_1(x) = \psi_2(x) \equiv 1. \tag{7}$$

By composition of (5) and (6) we obtain an equation for evolution over F_{k+2} steps of discrete time. With account of terms up to the first order in ε it reads

$$x_{i+F_{k+2}} = \phi_k(\phi_{k+1}(x_i)) + \varepsilon[\xi_i\phi_k'(\phi_{k+1}(x_i))\psi_{k+1}(x_i) + \xi_{i+F_{k+1}}\psi_k(\phi_{k+1}(x_i))]. \tag{8}$$

In respect to the stochastic term, we make the following remark. Let us suppose that at some moment an orbit starts at x_i. Consider an ensemble of the random numbers $\{\xi_i,\xi_{i+\mathrm{Fk+1}}\}$ of zero mean and mean square σ^2, and compose them with coefficients given by functions of x_i. As $\{\xi_i,\xi_{i+Fk+1}\}$ are statistically independent, the sum can be represented again as a random number of zero mean and of mean square σ^2, multiplied by a function of x_i, namely,

$$\xi_i\phi'_k(\phi_{k+1}(x_i))\psi_{k+1}(x_i)+\xi_{i+F_{k+1}}\psi_k(\phi_{k+1}(x_i))=\tilde{\xi}_i\psi_{k+2}(x_i). \tag{9}$$

Now, we introduce

$$\phi_{k+2}(x)=\phi_k(\phi_{k+1}(x)) \tag{10}$$

and rewrite Eq. (10) in the form analogous to (7) and (8), with redefined random variable and functions ϕ and Ψ

$$x_{i+F_{k+2}}=\phi_{k+2}(x_i)+\varepsilon\tilde{\xi}_i\psi_{k+2}(x_i). \tag{11}$$

To obtain closed functional equations, we square both parts of Eq. (9) and perform averaging over ensemble of realizations of the random variable. As $\left\langle\tilde{\xi}_i^2\right\rangle=\left\langle\xi_i^2\right\rangle=\sigma^2$, and $\left\langle\xi_i\xi_{i+F_{k+1}}\right\rangle=0$, we come to the relation

$$[\psi_{k+2}(x)]^2=[\phi'_k(\phi_{k+1}(x))]^2[\psi_{k+1}(x)]^2+[\psi_k(\phi_{k+1}(x))]^2, \tag{12}$$

where prime designates a derivative.

In accordance with the basic content of the renormalization approach, we implement now a scale change $x\mapsto x/\alpha^k, u\mapsto(-w)^k u$, where $\alpha=-1.288574553954368\ldots$ is the scaling constant for the critical golden mean dynamics [6,22]. Then, in terms of the rescaled functions

$$\begin{aligned} g_k(x)&=\alpha^k\phi_k(\alpha^{-k}x),\quad f_k(x)=\alpha^k\phi_{k+1}(\alpha^{-k}x),\\ \Phi_k(x)&=[\psi_k(\alpha^{-k}x)]^2,\ \Psi_k(x)=\alpha^k[\psi_{k+1}(\alpha^{-k}x)]^2, \end{aligned} \tag{13}$$

the above equations imply that

$$\begin{aligned} g_{k+1}(x)&=\alpha f_k(x/\alpha),\\ f_{k+1}(x)&=\alpha g_k(f_k(x/\alpha)),\\ \Phi_{k+1}(x)&=\alpha^2\Psi_k(x/\alpha),\\ \Psi_{k+1}(x)&=\alpha^2\{[g'_k(f_k(x/\alpha))]^2\Psi_k(x/\alpha)+\Phi_k(f_k(x/\alpha))\}. \end{aligned} \tag{14}$$

These relations define the RG transformation for a set of functions $\{g_k,f_k,\Phi_k,\Psi_k\}$. The procedure may be repeated again and again to get the functions for larger and larger k, i.e. to determine the renormalized evolution operators for larger Fibonacci's numbers of steps of discrete time F_k.

As follows from the RG analysis [6], at the GM critical point, the sequence of functions $g_k(x)$, $f_k(x)$ converges asymptotically to a fixed-point solution of the RG equation, a functional pair $\{g,f\}$, which obeys

$$g(x)=\alpha f(x/\alpha),\ f(x,y)=\alpha g(f(x/\alpha)) \tag{15}$$

or

$$g(x) = \alpha^2 g(\alpha^{-1} g(x/\alpha)). \tag{16}$$

Numerical data for polynomial expansion of the universal function $g(x)$ over powers of x^3 are known and may be found e.g. in Ref. [25].

Convergence of the sequence $\{g_k(x), f_k(x)\}$ to the fixed-point solution of the RG transformation implies that the recursive linear functional equations for the functional pairs $\{\Phi_k(x), \Psi_k(x)\}$ asymptotically correspond to a k-independent linear operator, and behavior of the solution is determined by an eigenvector associated with the largest eigenvalue Ω for this operator [16]:

$$\Omega \begin{pmatrix} \Phi \\ \Psi \end{pmatrix} = \begin{pmatrix} \alpha^2 \Psi(x/\alpha) \\ \alpha^2 \{[g'(f(x/\alpha))]^2 \Psi(x/\alpha) + \Phi(f(x/\alpha))\} \end{pmatrix}. \tag{17}$$

As mentioned, the universal functions $g(x)$ and $f(x)$ have been obtained in computations via accurate approximation by finite expansions over powers of x^3 [6,25]. Using those data, we constructed the functional transformation of the right-hand part of Eq. (17) as a computer program. The unknown functions $\{\Phi(x), \Psi(x)\}$ were represented by a set of their values at nodes of a grid on interval $-1.2 < x < 1.2$, and by an interpolation scheme between them. Taking arbitrarily initial conditions $\Phi(x) \equiv 1$, $\Psi(x) \equiv 1$, the program performed the functional transformation many times and normalized the resulting functions at each step as $\Phi^0(x) = \Phi(x)/\Phi(0)$, $\Psi^0(x) = \Psi(x)/\Phi(0)$, until the form of the functions stabilized. The value of $\Phi(0)$ (before the normalization) converges to the eigenvalue

$$\Omega = 5.318\,490\,477\,71\ldots \tag{18}$$

Now, for large k in linear approximation in the noise amplitude, the stochastic maps for evolution over F_k and F_{k+1} steps at the GM critical point may be written in terms of the renormalized variables as

$$\begin{aligned} x_{i+F_k} &= g(x_i) + \varepsilon \gamma^k \xi_i \varphi(x_i), \\ x_{i+F_{k+1}} &= f(x_i) + \varepsilon \gamma^k \xi_i v(x_i), \end{aligned} \tag{19}$$

where

$$\varphi(x) = \sqrt{\Phi^0(x)},\ v(x) = \sqrt{\Psi^0(x)},\ \gamma = \sqrt{\Omega} = 2.306\,185\,265\,26. \tag{20}$$

Next, let us consider a small shift of parameters r and K from the GM critical point. Then, some additional perturbation terms will appear in the equations, which correspond to two relevant eigenmodes of the RG equation linearized at the fixed point solution (see [6,25]). With account of them we write

$$x_{i+F_k} = g(x_i) + C_1 \delta_1^k h_q^{(1)}(x_i) + C_2 \delta_2^k h_q^{(2)}(x_i) + \varepsilon \gamma^k \xi_i \varphi(x_i), \tag{21}$$

where $h_1^{(1)}(x)$ and $h_1^{(2)}(x)$ are respective egenfunvectors. The eigenvalues δ_1 and δ_2, as found numerically [6,22], are

$$\delta_1 = -2.833610655891,\ \delta_2 = \alpha^2 = 1.660424381098. \tag{22}$$

Coefficients C_1 and C_2 in Eq. (21) depend on parameters of the original map and vanish at the critical point GM. In a close neighborhood of the critical point it is sufficient to account only leading terms of the power expansions in respect to deflections of the original parameters. The mode associated with C_1 corresponds to a shift along the critical line $K = 1$; the map retains the cubic inflection under this perturbation. The second mode, with coefficient C_2, appears due to a shift from the critical line along the curve of constant winding number. In accordance with Ref. [25], expressions for the coefficients C_1 and C_2 via parameters of the original sine circle map may be written as follows:

$$r - r_c = C_1 - 0.01749C_2 - 0.00148C_2^2,\ k - k_c = C_2.$$

We regard C_1 and C_2 as special local coordinates ("scaling coordinates") in a neighborhood of the GM critical point in the parameter plane.

Now, we are ready to formulate the basic scaling property of dynamics near the GM critical point in presence of noise that follows from (21).

If we have some parameter shift from the GM critical point and decrease it in such way that the coefficients C_1 and C_2 reduce by factors δ_1 and δ_2, respectively, and reduce noise amplitude ε by factor γ, then the form of the stochastic map (21) remains unchanged. Thus, at the new parameters, the noisy system will demonstrate statistically similar behavior as that with the old ones, but with a characteristic time scale increased by factor $F_{k+1}/F_k \cong w^{-1} = (\sqrt{5}+1)/2$.

4. Scaling properties and their demonstration in numerical computations

Let us discuss some manifestations of the effects of noise on the circle map at the GM critical point and in its vicinity in numerical experiments, in a frame of scaling regularities outlined in the previous section.

4.1. Noisy critical attractor

To examine scaling properties of the critical orbit at the GM point it is convenient to represent the motion in coordinates x_{n+F_k} versus x_n as done in Section 2, at subsequent Fibonacci numbers F_k.

First, we demonstrate in Fig. 3 the scaling property of the noiseless critical orbit. Inset in each picture shows a fragment of it, and these fragments are pictured with magnification increasing by factor $\alpha = -1.2885\ldots$ from one to another picture. Observe nice similarity of these rescaled plots. (Formally speaking, in accordance with RG analysis, this self-similarity is asymptotic: it become precise only at large k and for asymptotically small scales.) In the central diagram (b) the inset is pictured upside down because of negativity of the scaling factor α.

In presence of noise, a subtle structure of the critical quasiperiodic orbit is smeared out level by level, as the intensity of noise grows. In accordance with conclusions of the previous section, each new level blurs out as we increase magnitude of the noise source by factor $\gamma = 2.30618\ldots$ Diagrams in Fig. 4 show portraits of the noisy

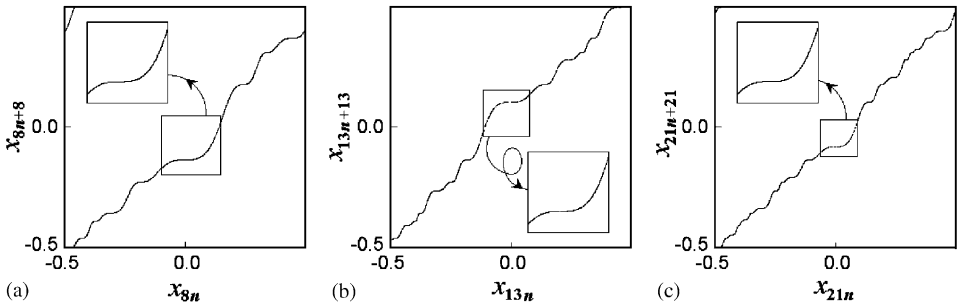

Fig. 3. Illustration of scaling for the golden-mean critical orbit in coordinates x_{n+F_k} versus x_n, $F_k = 8$, 13, 21 without noise. In each next picture an inset shows a fragment with magnification increased by $\alpha = -1.2885\ldots$ in comparison with the previous picture.

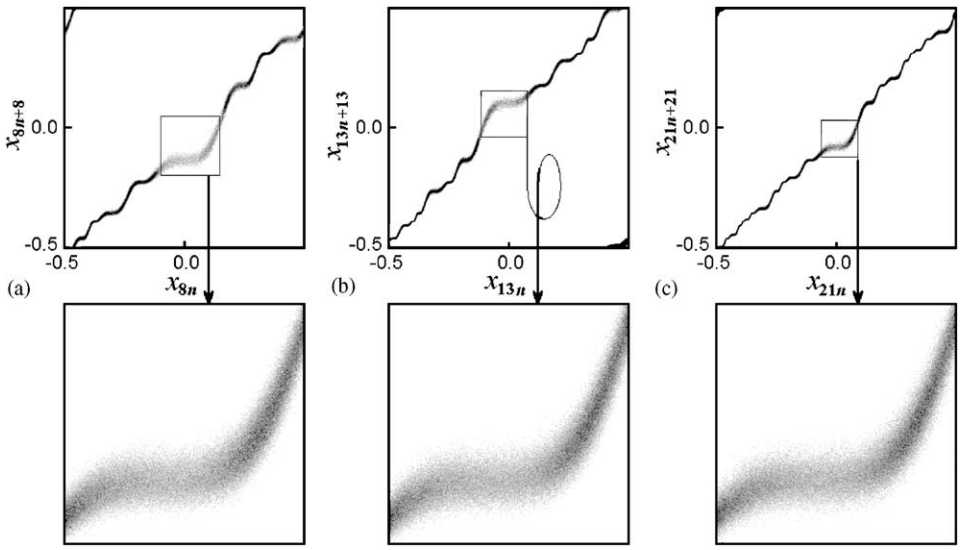

Fig. 4. Portraits of the orbit of the noisy circle map (3) at the GM critical point $r = r_c = 0.606661\ldots$, $K = 1$ at the noise amplitude values $\varepsilon = 0.005$ (a), $\varepsilon = 0.005/\gamma$ (b), and $\varepsilon = 0.005/\gamma^2$ (c).

attractors of the model system (3) at the GM critical point with the noise intensity parameter $\varepsilon = 0.005$ (a), $\varepsilon = 0.005/\gamma$ (b), and $\varepsilon = 0.005/\gamma^2$ (c). The right-hand panels represent boxes from the previous diagrams, with magnification for the plots (a), (b) and (c) with factors C, αC, and $\alpha^2 C$, respectively, where C is some constant. Observe similarity of the pictures for the noisy attractors.

4.2. Lyapunov exponent in the presence of noise

In accordance with results of Section 3, at the GM critical point the system will demonstrate similar behaviors for noise intensity values ε and ε/γ, and in the second

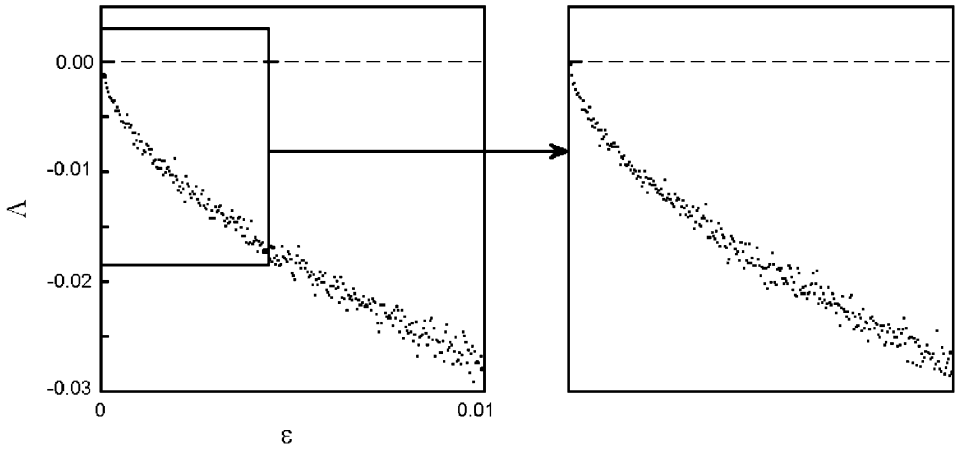

Fig. 5. Plots for the Lyapunov exponent versus the noise intensity ε. A selected box is shown with magnification by a factor $W = 1.618\ldots$ along the vertical axis, and by a factor $\gamma = 2.30618\ldots$ along the horizontal axis.

case characteristic time scale is larger by factor $W = w^{-1} = 1.6180\ldots$. Hence, magnitude of the Lyapunov exponent at ε/γ must be less than that at ε by this factor. Fig. 5 shows plots for the Lyapunov exponent versus the noise intensity ε. A selected box is shown with magnification by factor W along the vertical axis, and by factor γ along the horizontal axis. Observe self-similarity of the pictures under this scale change.

Let us estimate a critical index for the Lyapunov exponent with respect to the intensity of noise. As we know, a change of ε by factor γ is accompanied with a change of Lyapunov exponent by factor W. Thus, it must behave as

$$\Lambda \propto \varepsilon^{\eta}, \tag{23}$$

where $\eta = \log_{\gamma} W = 0.575\,891\,387...$ Fig. 6 shows dependence for Λ of ε in double logarithmic scale. The points obtained in the numerical computations are clearly placed along the straight line with slope η.

It is worth noting a kind of noisy stabilization of the dynamics at the GM point. Indeed, the noise promotes a decrease of the Lyapunov exponent, i.e. a decrease of sensitivity in respect to the initial conditions, and delays the onset of chaos. The same conclusion was mentioned in Refs. [14,21]. It is opposite to situation in the case of period-doubling transition to chaos [26].

4.3. Scaling regularities for a neighborhood of the critical point in presence of noise

Now let us turn to examination of scaling regularities in the circle map observed with detuning of the control parameters from the GM critical point.

Let us start with consideration of variation of one parameter r with constant $K = 1$. It implies that the map retains the cubic inflection point. In the perturbed

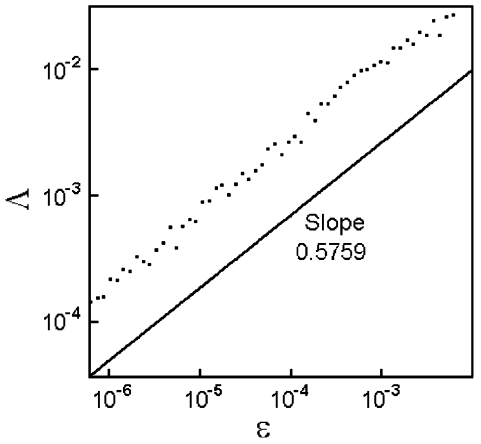

Fig. 6. Plot of the Lyapunov exponent versus noise intensity at the GM critical point in double logarithmic scale (dots). The straight line corresponds to the relation (23).

universal evolution operator (21) a shift of r gives rise to the mode with eigenvalue $\delta_1 = -2.83361...$,, and this universal number will present in the scaling relations.

Fig. 7 illustrates the corresponding scaling property of the dynamics without noise. The central diagram shows the rotation number dependence on parameter r:

$$\rho(r) = \lim_{n\to\infty} \frac{x_n}{2\pi n}. \tag{24}$$

(In the computation of ρ the modulus operation is ignored in the main Eqs. (1) or (3).)

The pictured object is known as "devil's staircase" [27]. It has infinite number of steps, each placed at a rational value of the rotation number. Steps correspond to crossing Arnold's tongues and to periodic motions. Growth of $\rho(r)$ takes place on a rest fractal set of parameter values associated with irrational rotation numbers, i.e., with quasiperiodic motions. At $K = 1$ this set has zero measure on axis r ("complete devil's staircase" [27]). The golden mean rotation number occurs just at the parameter r_c associated with the critical point under study. Panels to the left and to the right from the main central diagram of Fig. 7 show details of the staircase structure in a vicinity of the GM point. The property of self-similarity consists in reproduction of the structure in small scales under magnification by factor δ_1 along the horizontal axis and by factor $(-W^2) = -2.6180\ldots$ along the vertical axis.

In presence of noise, the rotation number may be determined in numerical simulations via the formula (24) in the same way as in a noiseless case, as an average over a large number of iterations. In the noisy system, however, we cannot speak of periodicity or quasiperiodicity in usual pure sense. Nevertheless, some crude classification remains yet possible.

At some values of r one can observe relatively long time intervals of dynamics close to periodic. These intervals alternate with rare noise induced "phase slips",

where the variable x accepts a relatively fast positive or negative shift approximately by a unit. These are, to say, motions representing a noisy version of periodicity. At other values, the variable x evolves without notable plateaus in the temporal dependence, with statistically well-defined trend. It corresponds to a noisy version of quasiperiodicity.

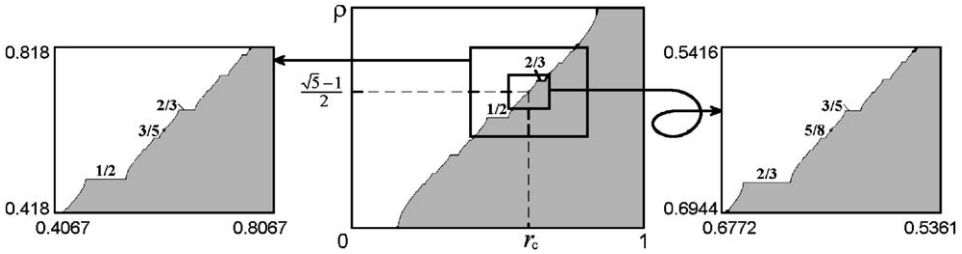

Fig. 7. Illustration of the local scaling property in a vicinity of the golden mean critical point without noise: a plot of rotation number ρ versus parameter r ("devil's staircase"). Property of self-similarity consists in reproduction of the structure in small scales under magnification by factor $\delta_1 = -2.8336$ along the horizontal axis, and by factor $(-W^2) = -2.6180\ldots$ along the vertical axis.

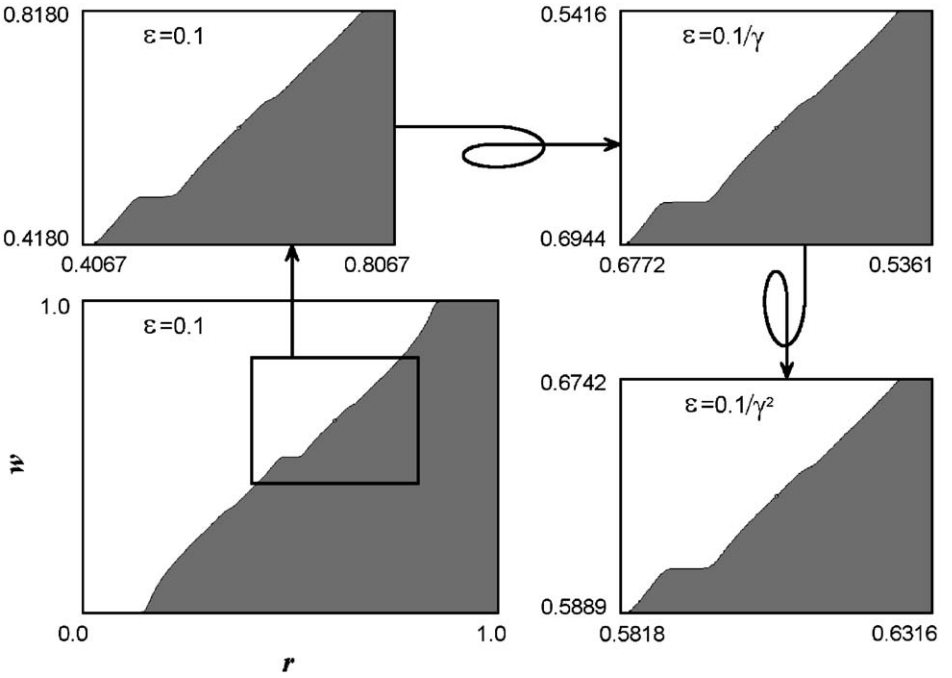

Fig. 8. Illustration of scaling in the structure of devil's staircase near the golden mean critical point in presence of noise. The main diagram and the first inset correspond to the noise level $\varepsilon = 0.1$. The subsequent pictures in order shown by arrows are plotted for noise intensities, respectively, $\varepsilon = 0.1/\gamma$ and $0.1/\gamma^2$.

On a plot of rotation number versus parameter r the picture looks like sequential smoothing out of the finest and than of larger and larger scale details of the fractal structure of devil's staircase. This phenomenon obeys the scaling property following from the RG analysis, as illustrated in Fig. 8. The main diagram and the first inset correspond to the noise level $\varepsilon = 0.1$. The second and the third pictures in the series (see arrows) are plotted for the noise levels $\varepsilon = 0.1/\gamma$ and $0.1/\gamma^2$, respectively. Observe obvious good correspondence of the visible structures in the three outside panels.

Fig. 9 shows a set of gray-scale Lyapunov charts on a plane of parameter r versus noise intensity ε at $K = 1$. Dark gray areas correspond to large negative values of the Lyapunov exponent. These are domains of "noisy periodicity", which gradually blur out with increase of noise. Light gray areas correspond to small negative Lyapunov exponent. These are domains of "noisy quasiperiodicity".

Finally, let us allow variation of two control parameters r and K in the stochastic circle map (3) and examine scaling properties of the picture of the noisy Arnold tongues.

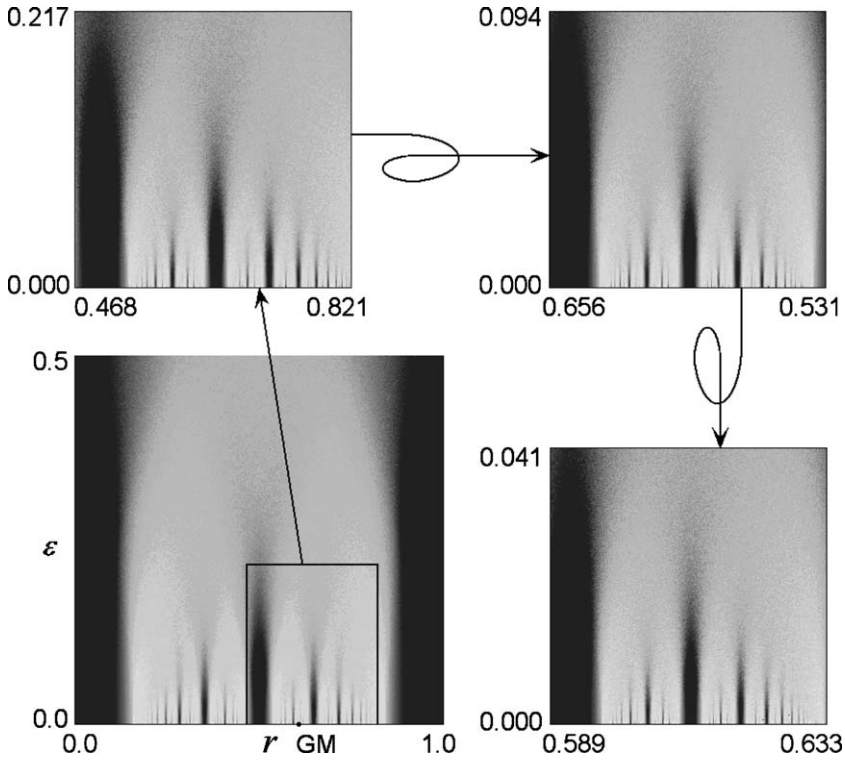

Fig. 9. Lyapunov charts demonstrating scaling in a neighborhood of the GM critical point at constant critical value of $K = 1$ on a plane of parameter r and noise amplitude ε. Horizontal and vertical scales in a sequence of diagrams in order indicated by arrows are subsequently changed, respectively, by factors $\delta_1 = -2.8336$ and $\gamma = 2.30618$. Simultaneously gray scale coding is redefined at each new level of magnification to make the similarity clearly visible.

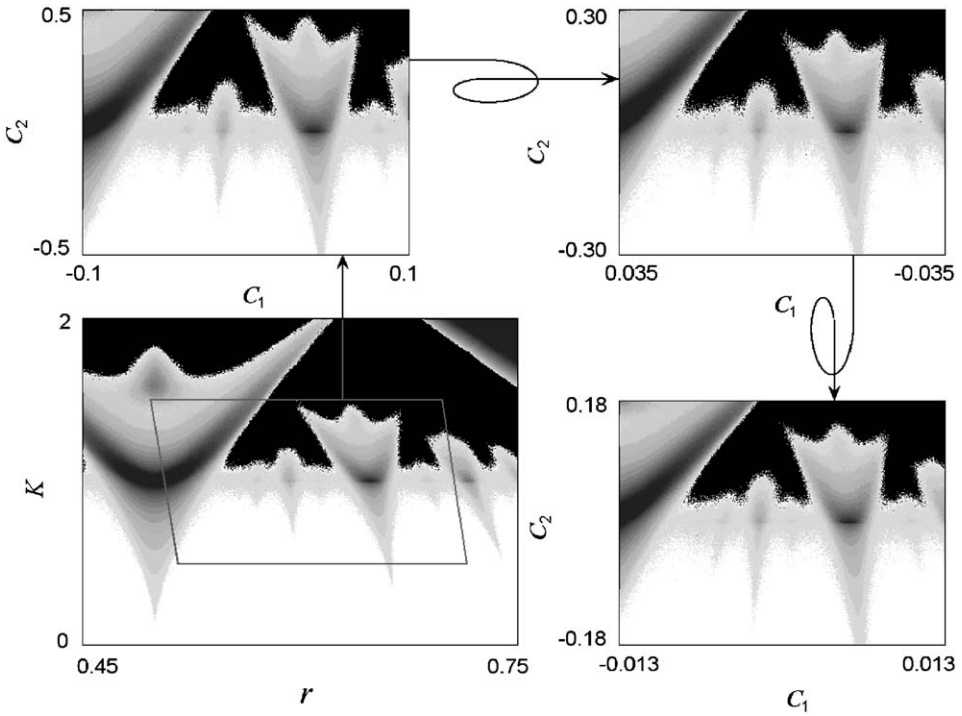

Fig. 10. Lyapunov charts demonstrating scaling in a neighborhood of the GM critical point. Rules of the gray scale coding are the same as in Fig. 1. The main diagram (a) plotted in coordinates (r, K) corresponds to the noise level $\varepsilon = 0.03$. Interior of a curvilinear quadrangle is shown separately (b) in scaling coordinates (C_1, C_2). On panels (c) and (d) horizontal and vertical scales are subsequently changed by factors $\delta_1 = -2.83361...$ and $\delta_2 = 1.66042...$, respectively, and the noise level is decreased by factor $\gamma = 2.30618...$ Gray scale coding is analogous to that in Fig. 1 and redefined at each new level of magnification to make the similarity clearly visible.

In Fig. 10 the main diagram shows a gray-scale Lyapunov chart for a part of the parameter plane with noise amplitude $\varepsilon = 0.03$. A curvilinear quadrangle in the diagram is bounded by coordinate lines of the scaling coordinates (22). The critical point GM is disposed exactly in the middle of the quadrangle. Its interior is shown in the first inset in the scaling coordinates. The next panels represent smaller and smaller vicinities of the critical point with subsequent decrease of the noise intensity by factor γ. Observe evident similarity of the pictures under several steps of the rescaling.

5. Conclusion

In this article we considered scaling regularities associated with the effect of additive noise on a sine circle map near the critical point of transition to chaos via the quasiperiodic motion with the golden-mean rotation number. On a basis of the

renormalization group approach we formulated several scaling relations and demonstrated them in numerical computations. In particular, we put attention to smearing due to the presence of noise of small-scale structure of the critical orbit, of devil's staircase, and of the noisy Arnold tongues.

It may be conjectured that the stated regularities are valid not only for a sine circle map, but for the entier universality class of nonlinear dissipative systems with quasiperiodic dynamics, which it represents. This assertion follows from the ideology of the RG approach. Thus, the same regularities will be intrinsic e.g. for self-oscillators and rotators under external periodic force, Josephson junctions in microwave field, driven fluid convection etc. As expected, the results of the present research will be helpful in treatment of experimental results of observation and investigation of the onset of complex behavior in systems of different physical nature demonstrating transition to chaos via quasiperiodic motions.

Acknowledgement

The work has been performed under a partial support from Russian Foundation of Basic Researches (Grant 04-02-04011), from Max Planck Society and from Deutsche Forschungsgemeinschaft.

References

[1] L. Glass, J. Sun, Phys. Rev. E 50 (1994) 5077;
V.S. Anishchenko, Dynamical Chaos — Models and Experiments, Appearance, Routes and Structure of Chaos in Simple Dynamical Systems, World Scientific, Singapore, 1995.
[2] P. Bak, T. Bohr, M.H. Jensen, P.V. Christiansen, Solid State Commun 51 (1984) 231.
[3] T. Bohr, P. Bak, M.H. Jensen, Phys. Rev. A 30 (1984) 1970.
[4] P. Alstrøm, B. Christiansen, P. Hyldgaard, M.T. Levinsen, R. Rasmussen, Phys. Rev. A 34 (1986) 2220.
[5] V.I. Arnold, Chaos 1 (1991) 20–24;
L. Glass, M.R. Guevara, A. Shrier, R. Perez, Physica D 7 (1983) 89.
[6] M.J. Feigenbaum, L.P. Kadanoff, S.J. Shenker, Physica D 5 (1982) 370;
S. Ostlund, D. Rand, J. Sethna, E.D. Siggia, Physica D 8 (1983) 303.
[7] M.J. Feigenbaum, J. Stat. Phys. 19 (1978) 25;
M.J. Feigenbaum, J. Stat. Phys. 21 (1979) 669;
M.J. Feigenbaum, Physica D 7 (1983) 16.
[8] J.M. Greene, R.S. MacKay, F. Vivaldi, M.J. Feigenbaum, Physica D 3 (1981) 468;
E.B. Vul, Ya.G. Sinai, K.M. Khanin, Russ. Math. Surv. 39 (3) (1984) 1;
J.-M. Mao, J.M. Greene, Phys. Rev. A 35 (1987) 3911;
A.P. Kuznetsov, S.P. Kuznetsov, I.R. Sataev, Physica D 109 (1997) 91.
[9] B. Hu, J. Rudnik, Phys. Rev. Lett. 48 (1982) 1645;
J.E. Hirsch, M. Nauenberg, D.J. Scalapino, Phys. Lett. A 87 (1982) 391.
[10] R.S. MacKay, Physica D 7 (1983) 283;
J. Wilbrink, Nonlinearity 3 (1990) 567.
[11] A.I. Golberg, Y.G. Sinai, K.M. Khanin, Russ. Math. Surv. 38 (1983) 187;
P. Cvitanović, J. Myrheim, Phys. Lett. A 94 (1983) 329;
O.B. Isaeva, S.P. Kuznetsov, Regular Chaotic Dyn. 5 (2000) 459.

[12] S.P. Kuznetsov, Radiophys. Quant. Electron. 28 (1985) 681;
H. Kook, F.H. Ling, G. Schmidt, Phys. Rev. A 43 (1991) 2700;
S.-Y. Kim, Phys. Rev. E 49 (1994) 1745.
[13] J. Stavans, F. Heslot, A. Libchaber, Phys. Rev. Lett. 55 (1985) 596;
M.H. Jensen, L.P. Kadanoff, A. Libchaber, I. Procaccia, J. Stavans, Phys. Rev. Lett. 55 (1985) 2798;
Z. Su, R.W. Rollins, E.R. Hunt, Phys. Rev. A 36 (1987) 3515.
[14] M.J. Kajanto, M.M. Salomaa, Solid State Communications 53 (1985) 99.
[15] J.P. Crutchfield, M. Nauenberg, J. Rudnik, Phys. Rev. Lett. 46 (1981) 933;
B. Shraiman, C.E. Wayne, P.C. Martin, Phys. Rev. Lett. 46 (1981) 935.
[16] A. Hamm, R. Graham, Phys. Rev. A 46 (1992) 6323.
[17] G. Györgyi, N. Tishby, Phys. Rev. Lett. 58 (1987) 527.
[18] J.V. Kapustina, A.P. Kuznetsov, S.P. Kuznetsov, E. Mosekilde, Phys. Rev. E 64 (2001) 066207.
[19] G. Györgyi, N. Tishby, Phys. Rev. Lett. 62 (1989) 353.
[20] O.B. Isaeva, S.P. Kuznetsov, A.H. Osbaldestin, Phys. Rev. 69 (2004) 036216.
[21] M. Markosova, P. Markos, Phys. Lett. A 136 (1989) 369.
[22] T.W. Dixon, T. Gherghetta, B.G. Kenny, Chaos 6 (1996) 32;
R. de la Llave, N.P. Petrov, Exp. Math. 11 (2002) 219.
[23] D. Fiel, J. Phys. A: Math. Gen. 20 (1987) 3209;
S.-Y. Choi, E.K. Lee, Phys. Lett. A 205 (1995) 173.
[24] J. Rössler, M. Kiwi, B. Hess, M. Markus, Phys. Rev. A 39 (1989) 5954;
M. Marcus, B. Hess, Comput. Graphics 13 (1989) 553;
J.C. Bastos de Figueireido, C.P. Malta, Int. J. Bifurcation Chaos 8 (1998) 281;
A.P. Kuznetsov, A.V. Savin, Nonlinear Phenomena Complex Syst. 5 (2002) 296.
[25] N.Yu. Ivankov, S.P. Kuznetsov, Phys. Rev. E 63 (2001) 046210, http://www.sgtnd.narod.ru//science/alphabet/eng/goldmean/GM.htm.
[26] J.P. Crutchfield, J.D. Farmer, B.A. Huberman, Phys. Rep. 92 (1982) 42.
[27] M.H. Jensen, P. Bak, T. Bohr, Phys. Rev. A 30 (1984) 1960;
P. Alstrøm, M.T. Levinsen, D.R. Rasmussen, Physica D 26 (1987) 336.